# High Performance Piezocomposite Energy Harvesters by Constructing Bionic Ion Channels

*Cheng Li[1,4], Ying Yang[4,5], Yanxiao Wu[4] , Xiaoming Tao[2,3], Wei Chen[2,3] **

Cheng Li

[1] Nano Science and Technology Institute, University of Science and Technology of China, Suzhou 215123, P. R. China

Prof. Xiaoming Tao, Prof. Wei Chen

[2]Research Centre for Smart Wearable Technology，Institute of Textiles and Clothing, The Hong Kong Polytechnic University, Hung Hom, Kowloon, Hong Kong, P. R. China

[3]The Hong Kong Polytechnic University Shenzhen Research Institute, Shen Zhen, China

E-mail: weii.chen@polyu.edu.hk

Ying Yang, Yanxiao Wu, Cheng Li

[4]i-Lab, Suzhou Institute of Nano-Tech and Nano-Bionics, Chinese Academy of Sciences, Suzhou, 215123, P. R. China

Ying Yang

[5]Nanchang Research Institute, Suzhou Institute of Nano-Tech and Nano-Bionics, Chinese Academy of Sciences, Nanchang, 330000, P. R. China

Keywords: piezocomposite energy harvesters, low frequency mechanical energy harvesters, bionic ion channels, wearable energy harvesters and storage devices

**Abstract**

In recent years, the traditional piezoelectric energy harvesters lack of effective progress in the field of wearable energy, because the requirement of generating continuous alternating current is long-time and high-frequency pressure, which is exactly human mechanical energy does not have. In addition, traditional piezoelectric materials cannot obtain sufficient short-circuit current and power density to supply power due to the high impedance of its dielectric layer. Here, in order to solve the problem of carrier shortage in traditional piezoelectric materials, we implant ions in the piezo-layer, and construct internal bionic ion channels to promote ion transport. The piezocomposite energy harvesters achieve a short-circuit current of 13.3 μA at low-frequency pressure, which is two orders of magnitude higher than that of traditional piezoelectric generator. Besides, the double layer structure formed by ions and composite carbon electrode has natural energy storage characteristics. It is found that the open-circuit voltage of piezocomposite energy harvesters will gradually accumulate step by step under the condition of ultra-low frequency pressure, and a longer discharge window will be obtained. The piezocomposite devices can rapidly charge under a pressure of 20 N and 1 Hz to obtain an open-circuit voltage of 150 mV within 80 s. This mode of introducing carriers into the piezo-layer to improve the performance of the piezoelectric generator, could provide a promising strategy for piezoelectric materials to collect and store low-frequency human mechanical energy, and also provide a new idea for the application of

bionic mesoporous materials in the power supply field of wearable electronic devices.

## 1. Introduction

Portable and wearable electronic equipment has been greatly developed with the advent of the Internet era.[1-4] Flexible nanogenerators have become the current research focus because they can convert mechanical energy in human motion into electrical energy that can power wearable devices.[4-6] For example, piezoelectric nanogenerators[7-9] prepared by piezoelectric effect generated by charge center deflection of crystal dipoles in semi-crystalline piezoelectric polymers under stress can be widely used in wearable research fields as self-powered sensors. In addition, triboelectric nanogenerators based on triboelectric effect and electrostatic coupling effect have received great attention in recent years due to their wide selection of materials, light weight and stable voltage output.[10-12] In spite of this, many researchers have found in their research that piezoelectric nanogenerators and triboelectric nanogenerators, due to the lack of sufficient carriers in their power generation layer and the too small charge density,[13-17] seriously limit their further application in the wearable energy field and need to be solved effectively.

Researchers have made many efforts to solve the problem of low charge density of flexible nanogenerators. For example, surface modification,[17, 18] introduction of an external charge pump,[15, 19] and so on.[20-22] In principle, ions as stable charge carriers can be used in the electromechanical conversion process to increase the charge density inside the generator. Previous studies have successfully used ions as media for energy conversion. For example, the ion diode flexible electromechanical conversion device

prepared by changing the equilibrium state of the ion p-n junction can obtain a short-circuit current output of 1.13 μA $cm^{-2}$. [23] There is also a gel battery prepared by reverse electrodialysis using a high salinity hydrogel to produce a considerable output.[24] In addition, the self-charging supercapacitor[25, 26] and the self-charging battery[27, 28] which use the mechanical piezoelectric field to drive the ions to move not only provide new ideas for solving the shortage of internal carriers, but also effectively solves the problem that the traditional energy harvesting device is difficult to combine power generation and storage.

Here, we introduce ions into the piezoelectric layer to solve the problem of charge carrier shortage in the piezoelectric layer. Furthermore, we regard the improvement of ion mobility as an important part of improving the output of piezoelectric composite devices. For this, We built bionic ion channels in the traditional polyvinylidene fluoride (PVDF) piezoelectric film, filling ionic liquid into the piezoelectric film to form a quasi-solid piezoelectric electrolyte layer, which greatly improved the mobility of ions. We are inspired by the rapid transportation of inorganic salts by conduits in tree trunks.[29] The PVDF membrane with bionic ion channels（BICM）, which is similar to the radius of the conduits (10 μm), is grown from bottom to top by cryogenic induced phase separation(CIPS),[30] which will greatly improve the permeability and ionic conductivity of PVDF piezoelectric membrane. On the other hand, in order to better absorb the energy of ions, we compounded SWCNT on carbon felt to obtain carbon composite electrode. Carbon electrode is considered as an excellent adsorption electrode for ions due to its excellent conductivity and specific surface area.[31, 32] We

further improved its cavity through compounding with carbon felt, which is conducive to the entry and adsorption of ions. In short, we use ions as the medium of energy transmission to collect the electric energy generated by the piezoelectric layer, and then form an electric double layer near the electrode to convert the energy back into electric energy. The effective output charge density of the piezocomposite energy harvesters(PCEHs) device can reach 24.5 mC $m^{-2}$ at a low frequency pressure of 50 N, 0.1 Hz, and a short-circuit current output of 13.3 μA can be obtained. In addition, PCEHs can harvest and store energy under ultra-low frequency external pressure. Each single pressure can spur more ions to migrate to the electrode surface and form a double-layer structure, so that the open circuit voltage can show a stable step-by-step rise even under extremely low-frequency pressure. The open circuit voltage of the device can be increased to 150 mV in 80 s under 20 N, 1 Hz pressure. And we can further improve the open circuit voltage of the device by connecting more devices in series to power the wearable small devices. In a word, the introduction of ions into the piezoelectric layer not only enhances the current output performance of PCEHs, but also effectively stores the low-frequency power generated by the piezoelectric separator in the form of ion concentration difference due to its own structure of the electric double layer capacitor. Therefore, the device integrates power generation and storage, providing a new and reliable solution for harvesting low-frequency mechanical energy generated by human motion, and also providing a new idea for preparing high-output mechanical energy harvesting devices.

## 2. Results and Discussion

### 2.1. Design principle of PCEH

Figure 1 illustrates the design principle of the PCEH device. The device consists of a quasi-solid piezoelectric electrolyte layer, a composite carbon electrode, and a copper foil (Figure 1a). Under the condition of no external pressure (Figure 1b), the ions in the quasi-solid electrolyte inside the device are in equilibrium. When pressure is applied to the device (Figure 1c), the polarized BICM will generate a piezoelectric field. The anion and cation continue to migrate toward the ends of the electrode under the action of the piezoelectric field, and an electric double layer structure occurs in the vicinity of the carbon composite electrode, causing a potential difference across the electrodes (Figure 1d). When the pressure is removed, the ions in the vicinity of the composite carbon electrode are continuously desorbed from the composite carbon electrode under the action of Brownian motion and electrostatic force (Figure 1e), and are mixed to an equilibrium state in the quasi-solid electrolyte. During this process, the potential difference between the electrodes at both ends continues to decrease. This cycle actually completes the energy conversion of mechanical energy to electrical energy through ions.

## 2.2. Formation of internal array ion channels in piezo-layers and assembly of piezocomposite energy harvesting devices

As we know, the passage structure in the trunk of a tree is an important part of transporting materials,[33] in which conduits can efficiently transport inorganic salt ions from plant roots to the top of plants without any energy supply. Inspired by this fact, we designed the BICM prepared by dimethyl sulfoxide (DMSO) ice crystals grown from bottom to top. We prepared BICM by CIPS method (Figure 2a). PVDF-DMSO polymer solution is placed on a copper heat conducting plate cooled by liquid nitrogen. Firstly, DMSO in contact with the copper conduction table is supercooled rapidly, and the crystal nucleus is formed immediately. According to the principle of crystallization kinetics, as the nucleation grows along with the lateral transport of the material, the growth of the DMSO nucleus gradually squeezes the PVDF to form the channel wall. With the development of cooling, the solid-liquid surface of DMSO icicle moves up with the cooling direction, in this process, along with the occurrence of material transport (figure 2b). [34] At the end of the freeze growth, dense and regular DMSO ice crystal columns are produced inside the membrane. Then the membrane is placed in an ice water mixture. Since the freezing point of DMSO is 18 ℃, the ice crystal column can fully maintain its shape in the ice water mixture. With the entropy increase reaction of the release of DMSO-$H_2O$ interfacial energy, DMSO crystal column is fully exchanged with water and removed to obtain BICM (Figure 2c).

Figure 2 shows the details of bionic channels of BICM. It can be seen from the section SEM that there are a lot of bionic channels in BICM. These channels are regular and

complete. As the channels in BICM come from the natural growth of DMSO icicle, similar to the growth of trees, these channels should be connected up and down (Figure 3a). In addition, unlike other methods such as template method and self-assembly method, the porous membrane prepared by CIPS is not limited by the area and thickness of the membrane, and does not need additional steps. As mentioned in the above part about the growth of DMSO crystal nucleus, the side where BICM contacts the heat conduction table will form a very thin and dense layer due to the rapid decrease of temperature and the great supercooling of DMSO, so the formed DMSO crystal nucleus is very small, so the part where BICM contacts the copper surface will form a very thin and dense layer (Figure S1, in the Supporting Information). From the SEM of the surface in contact with copper, it can be seen that there are a large number of pores on the surface (Figure 3b), and we have reason to believe that these dense pores will be connected with the pores in the middle of the membrane. With the cooling process, when the solid-liquid interface crosses the dense layer, the dense layer acts as a kind of heat insulation layer, resulting in the decrease of cooling rate. The crystallization of DMSO tends to be stable. We can find in Figure 3c that there are a large number of regular channels on the surface contacting with air, which shows that the bionic ion channels in BICM are connected up and down.

In principle, we can change the diameter of DMSO ice crystal column by changing the content of DMSO, so as to change the size of bionic ion channel. As shown in Figure 3d, we set three concentrations of PVDF / DMSO solution, from which we can find that the higher the DMSO content, the larger the diameter of the bionic ion channel formed.

And at the concentration of 15 wt%, the channel formed was 9.6 μm. And the area distribution of the channel is mainly concentrated in 60-100 $\mu m^2$ (Figure S3, in supporting information), which was the closest to the diameter of the conduit in the tree. [29, 35] In addition, from figure S2 in the supporting information, it can be found that the cross section of bionic ion channel presents irregular polygon, and the channel is complete without fragmentation.

As a kind of piezoelectric separation membrane, the membrane must meet a certain degree of pressure stability. In order to show the properties of BICM, a kind of porous membrane was prepared by phase invertion method (Figure S4, in supporting information), which was used as reference sample. As a kind of piezoelectric separation membrane, we hope it can meet certain pressure stability. As shown in Figure 4a, PVDF itself has certain physical elasticity. The strain of BICM prepared by CIPS can reach 153%, which is much higher than that of porous PVDF prepared by phase transformation (54%). This may be related to the reduction of stress concentration by regular and dense bionic channels. AC impedance spectra of the PCEHs prepared based on BICM, including small semicircles (high frequency regions), Warburg diffusion lines (intermediate frequency regions), and capacitance lines (low frequency regions) (Figure 4b). The equivalent series resistance $R_b$ with the capacitor is 49.32 Ω, which indicates that the carbon composite electrode has good interface contact with the ionic liquid and the good electron conduction performance of the carbon composite electrode. The line of the low frequency region is approximately perpendicular to the Z' axis, indicating a good capacitive behavior of the PCEH based on BICM.

In fact, its permeability and ionic conductivity are excellent due to the microchannel structure inside the BICM. Compared with the comparative sample, the purely water flux sample prepared by the freeze-grown film sample of the same thickness without any load pressure was 7641 $Lm^{-2}h^{-1}$, while the pure water flux of the phase inversion membrane is only 539 $Lm^{-2}h^{-1}$. The frozen growth film is about 15 times pure water flux of the phase inversion film (Figure 4c), this indicates that the PVDF membrane with the ion channels that pass through the top and bottom is much better than the common phase inversion membrane. Test the AC impedance spectra of the two types of membranes in a battery case (using stainless steel disc as electrode，$EMIBF_4$ as electrolyte) (Figure 4d). The ionic conductivity of the CIPS film was calculated to be 0.66 S $m^{-1}$. This indicates that the macroporous PVDF membrane with regular arrangement of ion channels is more susceptible to ion conduction than the membrane after phase inversion (0.11 S $m^{-1}$).

In order to illustrate the charge discharge performance of pceh equipment, we tested the GCD curve of pceh equipment. The GCD curves of the PCEH at different current densities exhibit linear and symmetric behavior, indicating the capacitive and fast charge/discharge properties (Figure S5.b). The specific capacitance of the PCEH device was 18.8 $mFg^{-1}$ at 0.04 mA $cm^{-2}$(Equation 1). The suitability of this SCSPC device for supercapacitor applications was further estimated by examining its power and energy densities. The energy density of the SCSPC reached 16.32 $mWhkg^{-1}$ (Equation 2) at a power density of 3.92 $kWkg^{-1}$(Equation 3). In addition, from the CV curve exhibited by different scanning voltages (Figure S5.a), the CV curve is smooth

overall, indicating that there is no obvious redox reaction at the SWCNT electrode. The increase in the current range of the CV profile with an increase in scan rate from 5 to 50 $mVs^{-1}$ suggests the capacitive property of the PCEH.

We polarize BICM to prepare BICM with piezoelectric effect. The polarization conditions are shown in Figure S6,in supporting imformation. The electric field polarization is to regularly arrange the β crystal structure inside the PVDF film. Before the polarization, the β crystal structure inside the film has a disordered polarity position, and does not generate a large voltage signal when subjected to pressure (Figure S7, in supporting information). After polarization, the β-polar crystal structure is regularly arranged along the direction of the electric field, and a piezoelectric potential of up to about 2.5 V can be generated when subjected to cyclic mechanical stress. In fact, we can find from the XRD pattern of the film obtained after the polarization of the electric field (Figure S8, in supporting information) that the crystal structure in the BICM is dominated by the β crystal structure. In the previous description of freeze growth, we can understand that PVDF segments are subjected to the force of DMSO ice crystal columns during the formation of macroporous membranes, which is conducive to the full extension of PVDF molecular segments and the formation of β crystal structure. In addition, PVDF molecular segments in BICM are more prone to form β crystals under the environment of high temperature and polarization electric field provided by the polarization step.[36]

**2.3. Energy harvesting and energy storage characteristics of PCEH devices.**

Figure 5 illustrates the short-circuit current performance of the PCEH devices under cyclic pressure. it has been previously proved that PVDF membranes with through ion channels prepared by cryogenic induse phase separation have excellent permeability and ion conductivity, which is conducive to the migration of anion and cation in the intermediate layer of quasi-solid electrolyte. We have compared the short-circuit current output of polarized BICM membranes and the PCEH assembled by polarized common phase conversion membranes under the same pressure conditions (50N, 0.1 Hz). It can be clearly seen that the PCEH device assembled by BICM can generate a peak current of about 10 μA (Figure 5a), while the PCEHs prepared by common phase transition film only has a peak current of about 0.67 μA $cm^{-2}$, which indicates that this ordered array ion channel structure can effectively improve the ion migration rate, thus increasing the current output during pressing. On the other hand, We believe that the polarization electric field generated by the internal polarization BICM cannot be ignored in the performance of PCEH equipment. We assemble polarized BICM and unpolarized BICM into PCEH equipment. As shown in Figure 5b, when two groups of equipment are tested under the same pressure, it can be found that the PCEH of polarized BICM can generate 13.3 μm short-circuit current, which is much higher than that of unpolarized devises. This shows that the internal electric field has an obvious promoting effect on PCEH. In addition, we tested the short-circuit current difference of the PCEH under different pressures (Figure 5c). We can clearly find that the greater the applied pressure, the greater the generated short-circuit current signal. In the range of 10 N-100 N, the short-circuit current peak value is linearly related to the applied

pressure value.

Figure 6 shows the open circuit voltage output performance of PCEH device. First, in order to understand the role of ions in PCEH devices, we removed ions from PCEH as a comparison (Figure 6a). On the left is a comparison of the short-circuit currents of the two types of devices at low frequency. It is clear that the short-circuit current output of an ion-filled PCEHs (4.57 μA) is much larger than that of a piezoelectric device without ion filling (~0.01 μA). In fact, the power generation principle of piezoelectric materials is to use external pressure to change the structure of internal crystals and generate polarization. Its output current mainly comes from the induction of polarized electric field to electrode electrons. Due to its lack of movable carriers, its current output has always been at a low level. On the right is the comparison of the open circuit voltages of the two types of devices. Since the electric double layer structure is not strongly bound to ions, the cumulative voltage generated by PCEH under low frequency pressure(13.63 mV) is not as large as that of pure piezoelectric materials(84.94 mV). However, it is worth noting that the PCEH device with ions has capacitive performance, and the voltage generated by it is not completely released in the case of an open circuit. Each low frequency pressure can increase the voltage by about 6 mV. In fact, we can calculate the ion migration number caused by a single pressing through the short circuit current performance of low frequency pressing. It can be calculated (Equation 4, in supporting information) that ions of $3.68*10^{-6}$ coulombs can effectively migrate to the electrode for electric double layer reaction, and the PCEH can generate a voltage output of 9.79 mV (Equation 5, in supporting information) with an output power of about 61.97

$nW/cm^2$, which is not much different from the actual situation. We tested the open-circuit voltage output of the device at ultra-low frequencies (Figure 6b), and the device can gradually increase the voltage to 41.5 mV in 200 s at an ultra-low frequency of 0.1 Hz. We also tested the open circuit voltage performance of a PCEH device at 1 Hz (Figure 6c), which is about the same frequency as the human walking. The device's open circuit voltage continues to increase by 150 mV in 70 s at 20 N, 1 Hz continuous pressure. In addition, we tested the cyclic stability of the PCEH (Fig.6d). The PCEH was charged to 100 mV under a continuous external pressure of 20 N and 1 Hz, and then discharged at a current of -10 μA. There was no significant change in the charge and discharge cycle after 80 cycles, indicating that the device has good cycle stability. On the other hand, the device can obtain a discharge window of -10 μA for up to 36 s after continuous pressure, which proves that the device has considerable performance in energy generation and energy storage.

Because of the capacitance characteristic of PCEH, we tested several PCEHs in series to increase its open circuit voltage (Figure 7a). Five PCEHs in series were stimulated with 20 N, 1 Hz pressure in turn, and the open circuit voltage of the series device can reach 453 mV continuously. This provides ideas for PCEHs to further increase its open circuit voltage. To demonstrate the potential application of PCEHs, we connected 10 PCEHs in series and powered a green LED (Figure 7b). The LEDs are successfully illuminated by sequentially pressing a single device (1 Hz, 40 sec) in sequence. In addition, we designed a folding series of multiple PCEHs and implanted them inside the insole (Figure 7c). By applying a low-frequency pressure (0.2 Hz, 150 N) similar to

the foot movement of the human body, we can obtain an average peak short-circuit current of 29 μA and cause a continuous increase in the open circuit voltage of the PCEHs combination device.

## 3. Conclusion

In summary, the electric double layer structure formed by ions and composite carbon electrodes is the direct cause of the potential difference generated by the ele ctrodes. External mechanical energy is converted into electrical energy by polarized PVDF mesoporous membrane. The ions act as continuous carriers to convert the intermittent electric field energy into the potential energy of the difference between the anion and cation ions, and convert it into electric energy through the electric double layer structure. Due to the low electrical resistance and high charge density brought about by the internal flow of carriers in the quasi-solid electrolyte gel, our devices exhibit high output current compared to various energy harvesting devices that are currently being studied extensively (Table 1,in supporting information). The advantage of the double-layer structure of the carbon composite electrode is the rapid adsorption and desorption of ions, so the device can be charged in a short time. However, due to the special limitations of the ionic double layer structure, our devices have lower open circuit voltages than conventional piezoelectric ceramic and piezoelectric polymer devices. Nonetheless, we can increase the voltage output of the device by connecting multiple sets of devices in series, so that it can power a typical small wearable electronic device. In this work, a piezocomposite energy harvesters that integrates mechanical energy harvesting and energy storage is designed and assembled. The innovation lies in the

introduction of ionic liquids as removable carriers in conventional piezoelectric polymers, which greatly increases the surface charge density and short-circuit current output of piezoelectric generators. In addition, bionic ion channels prepared by cryogenic induced phase separation enhance ion migration rates. Composite nanogenerators can achieve an output surface charge density of up to 24.5 mC $m^{-2}$ and a short-circuit current of 13.3 μA. The device can obtain an open circuit voltage of 150 mV within 80 seconds under a low frequency pressure of 1 Hz. And we can choose to connect multiple devices in series to power small wearable electronic devices. This work provides a new idea for the development of high-power self-charging batteries with small charging time, and provides a new way to collect human body mechanical energy in low frequency state. In addition, This method of introducing carriers into the piezoelectric layer provides a new feasible scheme for the preparation of high-performance piezocomposite energy harvesters, which will contribute to the further application of piezoelectric materials in the wearable field.

## 4. Experimental Section

*Preparation of BICM by CIPS method*: PVDF powder (Sigma-Aldrich, Mw ca. 530,000) was fully dissolved in dimethyl sulfoxide（DMSO；Sigma-Aldrich, AR>99.9%）solvent (15 wt%) at 60℃.Drop 0.5 ml of polymer solution onto the copper heat-conducting plate, and fasten a rectangular Teflon frame (2×3 cm) around it to ensure a certain shape, and keep it for 5 min. Subsequently, liquid nitrogen is injected under the copper heat-conducting plate, and the polymer film solidified at low temperature is taken out of the copper heat-conducting plate after 5 min, and is put into an ice-water mixture for phase

conversion. The BICM is obtained after taking out the film and drying the moisture after 24 h.

*Polarize BICM:* The prepared membrane was placed in silicone oil and placed in a vacuum oven for 3 hours to remove air bubbles inside the ion channel. The temperature of silicone oil was kept at 100 ℃ and the membrane was placed in an electric field of 20 KV/mm for 1 h. Then it is placed in toluene for 12 h to remove residual silicone oil, and then the membrane is taken out of toluene and placed in an oven at 60 ℃ for 3 h so that toluene volatilizes completely. After that, we will obtain the BICM with piezoelectric properties as our piezoelectric separation membrane.

*Preparation of Carbon Composite Electrode:* 25 mg of single-walled carbon nanotubes (Nanjing XFNANO Materials Tech Co. Ltd. length~30μm) were placed in 10 ml of ethanol, and 25 mg of cellulose binder was doped into the single-walled carbon nanotubes after ultrasonic treatment for 45 min in an ultrasonic crusher. After stirring for 30min, the cut carbon fiber felt was immersed in the mixed solution of carbon nanotubes, and after 10 min, it was taken out and dried to obtain the carbon fiber felt - SWCNT- cellulose composite electrode.

*PCEH assembly:* Dipping BICM into EMIBF4 ionic liquid (Shanghai Chengjie Chemical Co. Ltd.), placing in a vacuum environment for 1 h to remove bubbles in the ion channel, taking out and drying excess ionic liquid on the surface. We will obtain a quasi-solid electrolyte intermediate layer. The carbon composite electrode is used to clamp the intermediate layer of the quasi-solid electrolyte, copper foil and PET are pasted on the outer layer, the remaining space is filled with PDMS and air is squeezed

out, and the PDMS is completely solidified in a 60 ℃ oven to obtain the PCEH.

*Preparation of phase inversion membrane comparison sample:* 15wt% PVDF-DMSO solution is evenly coated on a glass plate. Then immersed in pure alcohol for 6 hours, phase inversion to remove DMSO to form porous membrane. Taking out and putting into water to shape the PVDF porous membrane, then taking out and drying to obtain a common phase inversion membrane as a contrast sample.

*Characterization:* All the electrochemical characterizations were recorded by a CHI760D electrochemical work station. SEM and TEM images were recorded by Hitachi S-4800 and FEI Tecnai G2 F20, respectively. X-ray photoelectron spectra were obtained using PHI 5000 VersaProbe II instrument.

**Acknowledgements**

We thank the project 2018YFC2000900 supported by National Key R&D Program of China, the project 21975214 supported by National Natural Science Foundation of China, the project BE1H supported by Start-up Fund of Hong Kong Polytechnic University, the project BE2016086 supported by the Science and Technology of Jiangsu Province.

## References


[1] S. Jung, S. Hong, J. Kim, S. Lee, T. Hyeon, M. Lee, D. H. Kim, *Sci Rep.* **2015**, *5*, 9.

[2] S. Choi, S. Kwon, H. Kim, W. Kim, J. H. Kwon, M. S. Lim, H. S. Lee, K. C. Choi, *Sci Rep.* **2017**, *7*, 8.

[3] Z. M. Tian, J. He, X. Chen, Z. X. Zhang, T. Wen, C. Zhai, J. Q. Han, J. L. Mu, X. J. Hou, X. J. Chou, C. Y. Xue, *Nano Energy.* **2017**, *39*, 562.

[4] F. R. Fan, W. Tang, Z. L. Wang, *Adv. Mater.* **2016**, *28*, 4283.

[5] X. Pu, L. X. Li, M. M. Liu, C. Y. Jiang, C. H. Du, Z. F. Zhao, W. G. Hu, Z. L. Wang, *Adv. Mater.* **2016**, *28*, 98.

[6] Z. L. Wang, G. Zhu, Y. Yang, S. H. Wang, C. F. Pan, *Mater. Today.* **2012**, *15*, 532.

[7] V. Vivekananthan, A. Chandrasekhara, N. R. Alluri, Y. Purusothaman, W. J. Kim, C. N. Kang, S. J. Kim, *Mater. Lett.* **2019**, *249*, 73.

[8] Y. H. Sun, J. G. Chen, X. N. Li, Y. Lu, S. J. Zhang, Z. X. Cheng, *Nano Energy.* **2019**, *61*, 337.

[9] S. Siddiqui, H. B. Lee, D. I. Kim, L. T. Duy, A. Hanif, N. E. Lee, *Adv. Energy Mater.* **2018**, *8*, 11.

[10] Z. L. Wang, J. Chen, L. Lin, *Energy Environ. Sci.* **2015**, *8*, 2250.

[11] F. R. Fan, Z. Q. Tian, Z. L. Wang, *Nano Energy.* **2012**, *1*, 328.

[12] J. X. Zhao, H. Y. Li, C. W. Li, Q. C. Zhang, J. Sun, X. N. Wang, J. B. Guo, L. Y. Xie, J. X. Xie, B. He, Z. Y. Zhou, C. H. Lu, W. B. Lu, G. Zhu, Y. G. Yao, *Nano Energy.* **2018**, *45*, 420.

[13] S. H. Wang, L. Lin, Z. L. Wang, *Nano Energy.* **2015**, *11*, 436.

[14] Z. L. Wang, *Mater. Today.* **2017**, *20*, 74.

[15] W. L. Liu, Z. Wang, G. Wang, G. L. Liu, J. Chen, X. J. Pu, Y. Xi, X. Wang, H. Y. Guo, C. G. Hu, Z. L. Wang, *Nat. Commun.* **2019**, *10*, 9.

[16] X. Y. Wei, G. Zhu, Z. L. Wang, *Nano Energy.* **2014**, *10*, 83.

[17] S. H. Wang, Y. L. Zi, Y. S. Zhou, S. M. Li, F. R. Fan, L. Lin, Z. L. Wang, *J. Mater. Chem. A.* **2016**, *4*, 3728.

[18] G. Zhu, Z. H. Lin, Q. S. Jing, P. Bai, C. F. Pan, Y. Yang, Y. S. Zhou, Z. L. Wang, *Nano Lett.* **2013**, *13*, 847.

[19] S. H. Wang, Y. N. Xie, S. M. Niu, L. Lin, C. Liu, Y. S. Zhou, Z. L. Wang, *Adv. Mater.* **2014**, *26*, 6720.

[20] J. Wang, C. S. Wu, Y. J. Dai, Z. H. Zhao, A. Wang, T. J. Zhang, Z. L. Wang, *Nat. Commun.* **2017**, *8*, 8.

[21] L. Cheng, Q. Xu, Y. B. Zheng, X. F. Jia, Y. Qin, *Nat. Commun.* **2018**, *9*, 8.

[22] A. R. Chowdhury, A. M. Abdullah, I. Hussain, J. Lopez, D. Cantu, S. K. Gupta, Y. B. Mao, S. Danti, M. J. Uddin, *Nano Energy.* **2019**, *61*, 327.

[23] Y. Hou, Y. Zhou, L. Yang, Q. Li, Y. Zhang, L. Zhu, M. A. Hickner, Q. M. Zhang, Q. Wang, *Adv. Energy Mater.* **2017**, *7*, 6.

[24] T. B. H. Schroeder, A. Guha, A. Lamoureux, G. VanRenterghem, D. Sept, M. Shtein, J. Yang, M. Mayer, *Nature.* **2017**, *552*, 214.

[25] A. Ramadoss, B. Saravanakumar, S. W. Lee, Y. S. Kim, S. J. Kim, Z. L. Wang, *ACS Nano.* **2015**, *9*, 4337.

[26] K. Parida, V. Bhavanasi, V. Kumar, J. X. Wang, P. S. Lee, *J. Power Sources.* **2017**, *342*, 70.

[27] H. X. He, Y. M. Fu, T. M. Zhao, X. C. Gao, L. L. Xing, Y. Zhang, X. Y. Xue, *Nano Energy.* **2017**, *39*, 590.

[28] Y. S. Kim, Y. N. Xie, X. N. Wen, S. H. Wang, S. J. Kim, H. K. Song, Z. L. Wang, *Nano Energy.* **2015**, *14*, 77.

[29] S. M. Xu, C. J. Chen, Y. D. Kuang, J. W. Song, W. T. Gan, B. Y. Liu, E. M. Hitz, J. W. Connell, Y. Lin, L. B. Hu, *Energy Environ. Sci.* **2018**, *11*, 3231.

[30] Z. L. Yu, N. Yang, L. C. Zhou, Z. Y. Ma, Y. B. Zhu, Y. Y. Lug, B. Qin, W. Y. Xing, T. Ma, S. C. Li, H. L. Gao, H. A. Wu, S. H. Yu, *Sci. Adv.* **2018**, *4*, 10.

[31] M. F. L. De Volder, S. H. Tawfick, R. H. Baughman, A. J. Hart, *Science.* **2013**, *339*, 535.

[32] S. Park, M. Vosguerichian, Z. A. Bao, *Nanoscale.* **2013**, *5*, 1727.

[33] M. Notaguchi, S. Okamoto, *Front. Plant Sci.* **2015**, *6*, 10.

[34] T. Wu, W. Q. Zhang, Y. F. Li, Y. Zheng, B. Yu, J. Chen, X. M. Sun, *Adv. Energy Mater.* **2018**, *8*, 7.

[35] C. W. Windt, F. J. Vergeldt, P. A. De Jager, H. Van As, *Plant Cell Environ.* **2006**, *29*, 1715.

[36] P. Martins, A. C. Lopes, S. Lanceros-Mendez, *Prog. Polym. Sci.* **2014**, *39*, 683.

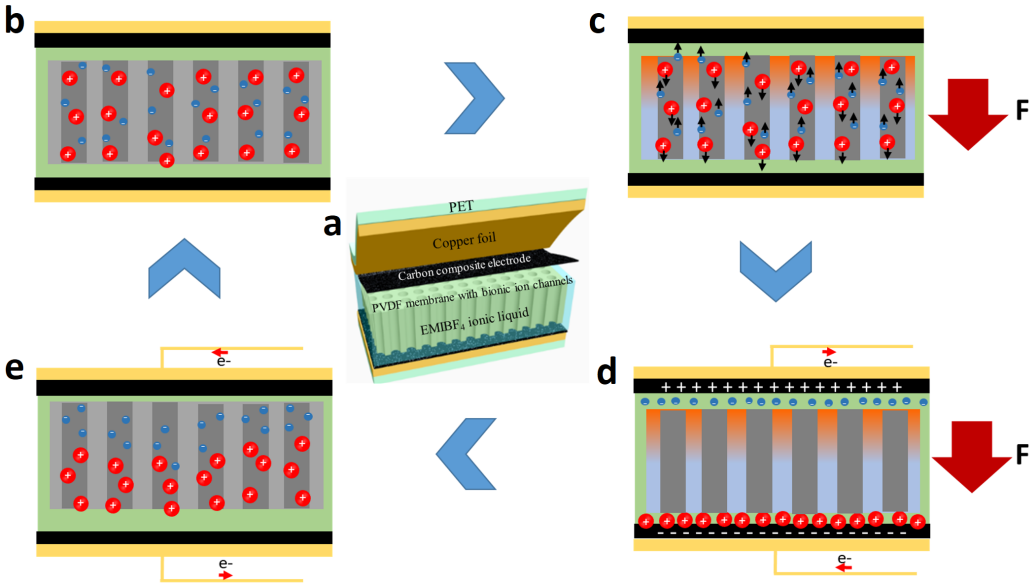


**Figure 1**. Principle of power generation of ion piezoelectric generator: a) Schematic diagram of the PCEH component. b) Ion distribution inside the device without external pressure. c) When the external pressure acts on the PCEH devices, the internal electric field is excited. d) Anions and cation migrated by the internal electric field. e) After the pressure is released, the ions are desorbed from the electrode and recombined within the BICM to reach equilibrium.

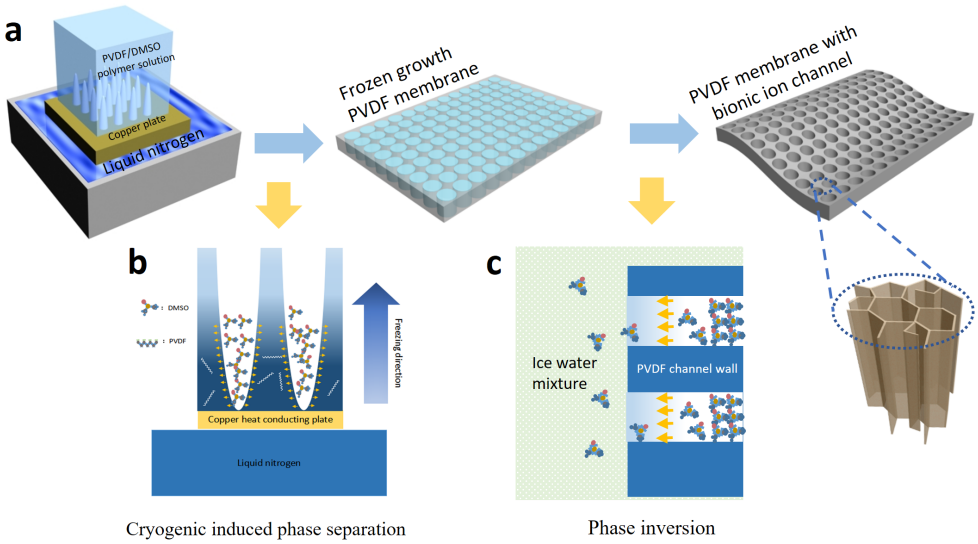


**Figure 2**. Formation of internal bionic ion channels: a) The PVDF membranes with bionic ion channels were preparation by cryogenic induced phase separation. b) Principle of cryogenic induced phase separation. c) Principle of phase inversion to remove DMSO crystal.

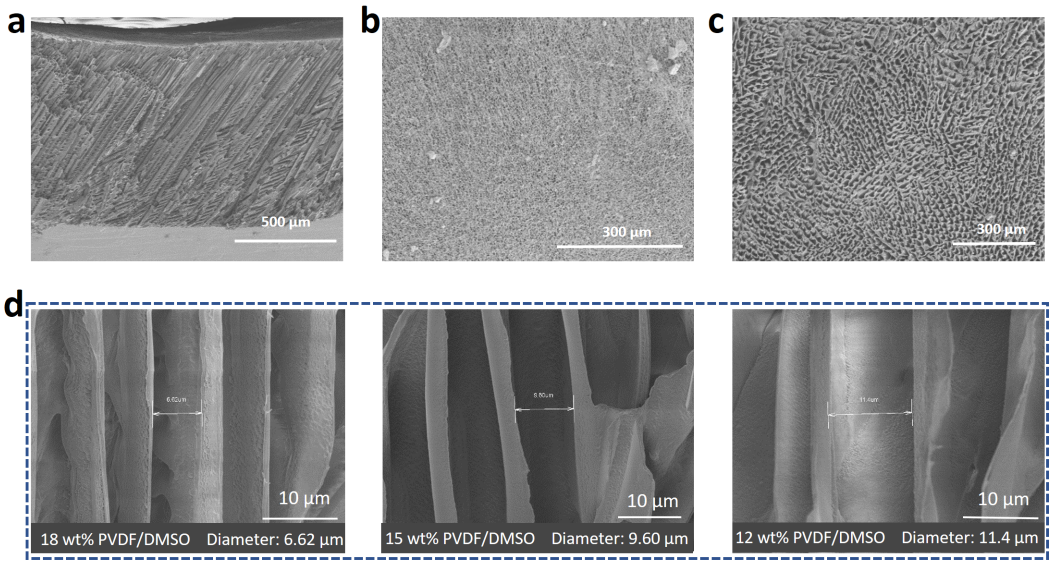


**Figure 3**. Morphological structure of BICM under scanning electron microscope: a) SEM image of cross section of BICM. b) SEM image of the surface of BICM in contact with thermally conductive copper. c) SEM image of BICM surface in contact with air. d) Variation of pore size of BICM membrane with solution concentration.

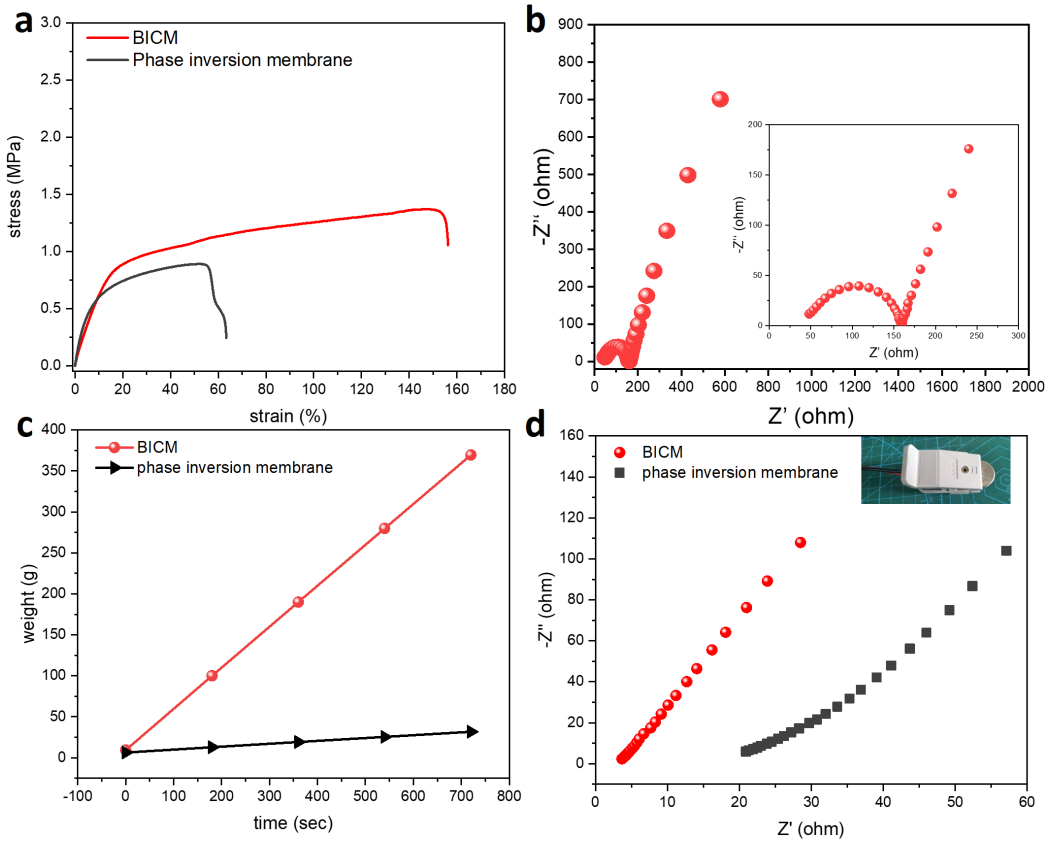


**Figure 4.** Transmission performance and ionic conductivity of BICM: a) Comparison of stress-strain curves between BICM and phase inversion membrane. b) Ac impedance spectrum of the PCEH, The inset shows the detail of high frequency area the detail. c) Comparison of pure water flux of BICM and phase inversion membrane. The temperature is 20 ° C, the additional pressure is 1 atm, and the sample thickness is 510 μm. d) Nyquist diagram of BICM and phase inversion membrane of the same thickness, the test electrode is a stainless steel electrode and the internal electrolyte is EMIBF4.

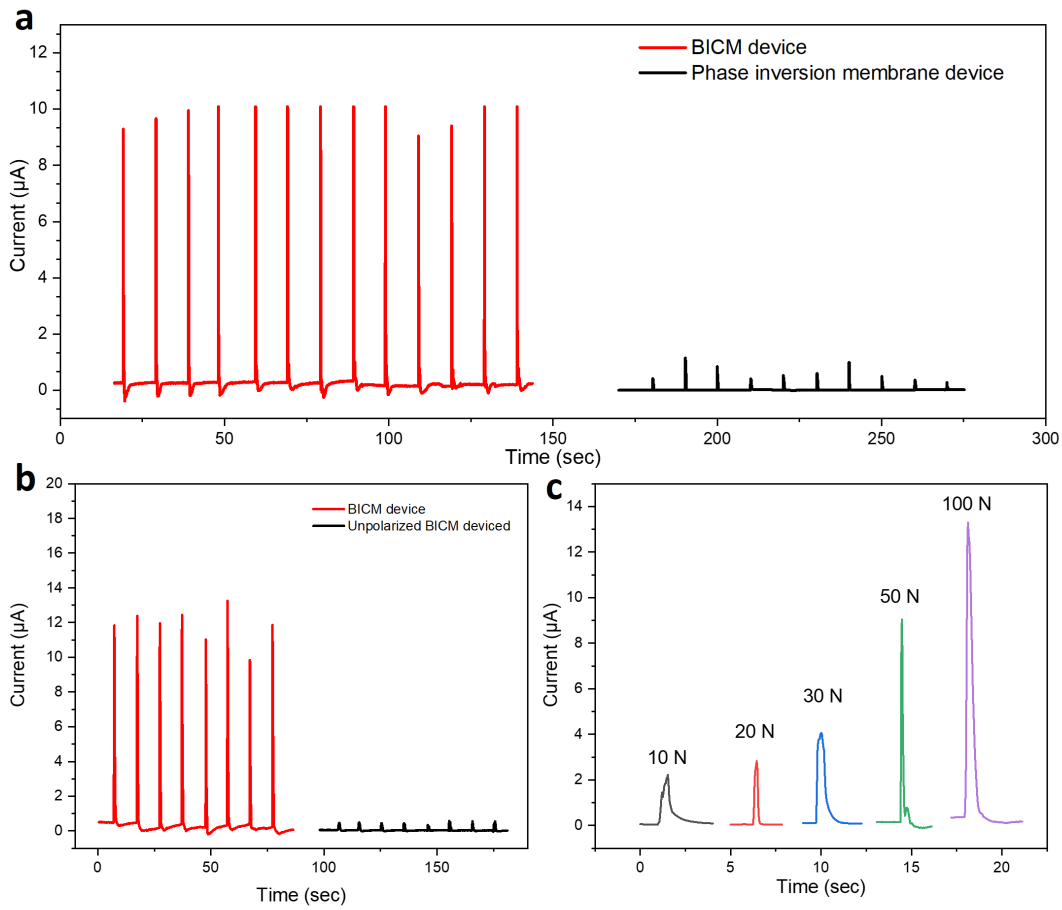


**Figure 5**. Short-circuit current output of PCEH and its influencing factors: a) Short-circuit current output comparison of polarized BICM devices and polarized phase-conversion membrane devices. Pressure:50 N, frequency:0.1 Hz . b) Comparison of short circuit current output between PCEH devices with and without electric field. Pressure:100 N, frequency:0.1 Hz. c) Short-circuit current performance of the PCEH under different pressures.

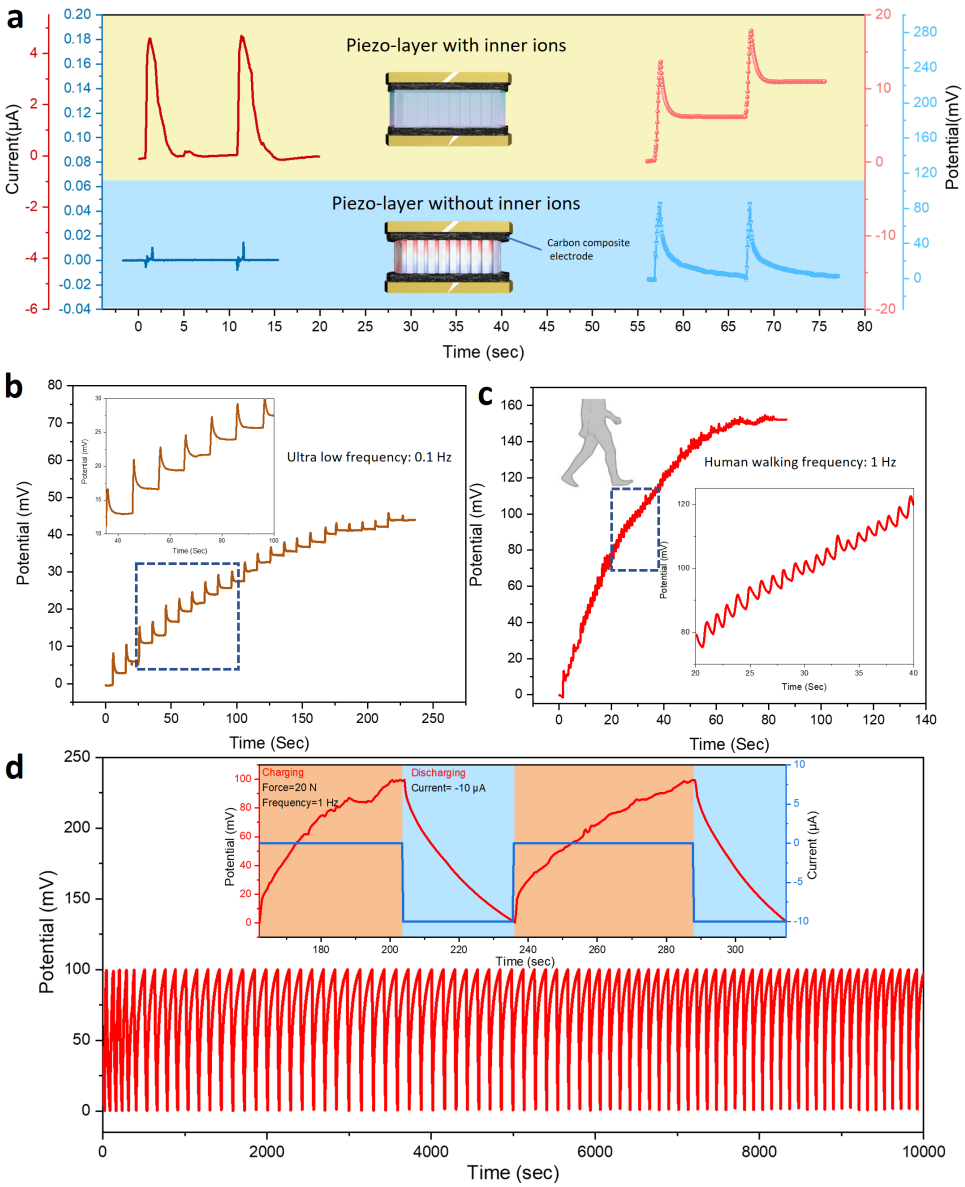


**Figure 6.** Energy harvesting and energy storage performance of PCEH devices: a) Comparison of open circuit voltage and short circuit current of PCEH devices with and without ions, Test pressure (0.1 Hz, 20N). b) Open circuit voltage performance of PCEH devices under ultra-low frequency (0.1 Hz, 20 N). c) Open circuit voltage performance of PCEH devices under human walking frequency (1 Hz, 20 N). d) The PCEH device charges and discharges multiple cycles, charging at 20N and 1Hz to 100mV and then discharging at a discharge current of 10 μA. The inset illustrates the details of the two cycles.

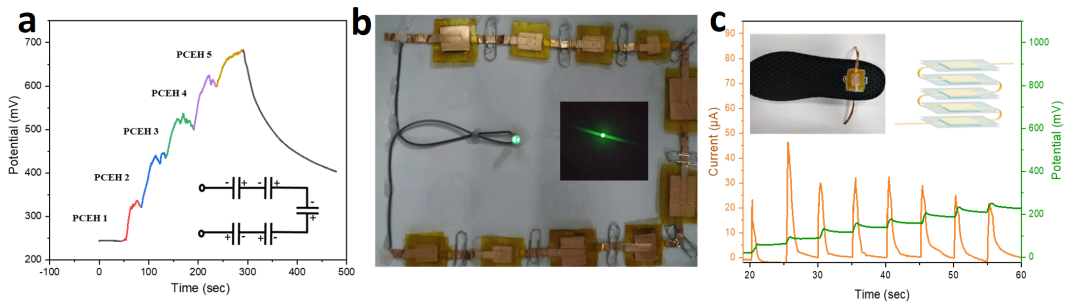


**Figure 7**. Application of PCEHs combined series device: a) Self-charging performance of series devices with continuously charging five series PCEHs devices. b) A green LED is powered by successively pressing the series of PCEHs. The inset shows the LED light in the dark environment. c) Performance of folded series PCEHs placed in the insole at low frequency pressure (Frequency=0.2 Hz, force=150 N). The inset shows optical photo of the combined device and it's internal connection structure diagram.